Santana Barros, K.; Martí Calatayud, MC.; Pérez-Herranz, V.; Espinosa, DCR. (2020). A three-stage chemical cleaning of ion-exchange membranes used in the treatment by electrodialysis of wastewaters generated in brass electroplating industries. Desalination. 492:1-11. https://doi.org/10.1016/j.desal.2020.114628

A three-stage chemical cleaning of ion-exchange membranes used in the treatment by electrodialysis of wastewaters generated in brass electroplating industries

Kayo Santana Barros[1]; Valentín Pérez-Herranz[2], Denise Crocce Romano Espinosa[3]

[1,3] Department of Chemical Engineering, University of São Paulo (USP). Address: Av. Professor Lineu Prestes, 580, Bloco 18 – Conjunto das Químicas, 05434-070. São Paulo – SP. Brazil.

[1,2] IEC Group, ISIRYM, Universitat Politècnica de València – Spain. Address: Camí de Vera s/n, 46022, P.O. Box 22012, València E-46071, Spain.

[1]Corresponding author: kayobarros@usp.br

[2] vperez@iqn.upv.es

[3] espinosa@usp.br

Abstract: After long-term electrodialysis, cleaning the membranes is crucial to extend their lifetime. In this work, we evaluate the effects of a three-stage chemical cleaning on electrochemical and structural properties of anion- and cation-exchange membranes. Membranes used in the electrodialytic treatment of a synthetic effluent from the cyanide-free brass electrodeposition were cleaned using 0.1, 0.5 and 1.0 mol·L^{-1} NaOH solutions. The electrochemical behavior of the membranes was evaluated after each cleaning step by chronopotentiometry. Additionally, changes in the membrane structure and composition were analyzed by FTIR-ATR and SEM/EDS. While the membranes undergo a decline in some electrochemical features after the electrodialysis process, the cleaning with 0.1 mol·L^{-1} NaOH showed to be the most effective in recovering the properties characteristic of the virgin membranes: the limiting current density increased by 84% after the cleaning, whereas the ohmic and overlimiting resistances decreased by 47% and 55%, respectively. In contrast, the 0.5 and 1.0 mol·L^{-1} NaOH solutions degraded the membranes and reduced their fraction of conductive area, especially for the anion-exchange one. This favored fouling/scaling occurrence, as noticed by a prominent increase in the potential drop of the anion-exchange membrane. FTIR-ATR and SEM/EDS analyses confirmed fouling/scaling, as well as degradation of the ion-exchange membranes.

Keywords: Membrane fouling; Membrane cleaning; Ion-exchange membranes; Alkaline cleaning; Chronopotentiometry.

1. Introduction

Electrodialysis (ED) is mostly used to produce drinking water. Additionally, this technology also finds application in other areas; such as the food industry [1,2], the treatment of industrial effluents [3,4] and the production of ultrapure water [5]. In the recent years, ED has been evaluated as a clean alternative to conventional techniques applied in the treatment of spent electroplating baths, like chemical precipitation or the use of ion-exchange resins [6]. Compared with conventional treatments applied in the management of effluents containing metallic ions, ED involves several advantages: (a) it is operated in continuous mode, (b) it does not need from regeneration steps neither involves the addition of further chemicals and, (c) it minimizes the generation of large volumes of waste sludge [7,8]. Instead of that, the products of the process are two liquid streams: one free of ionic species and the other one concentrated in valuable metals, which can be recycled into the electroplating process.

Within electroplating operations, cyanide-free electroplating has been intensively evaluated in the search for environmentally friendly alternatives that do not imply using highly toxic cyanide compounds. Recently, we assessed the replacement of cyanide by EDTA as complexing agent in the brass electroplating industry, and demonstrated that uniform, crack-free, and bright electrodeposits could be obtained [9]. Although cyanide is not present, the wastewaters generated during the brass electroplating still contain metallic impurities that need to be removed. In our previous work, the transport through heterogeneous anion-exchange membranes of complexes present in the spent EDTAbased brass electroplating effluent was evaluated [10]. In a subsequent study, a synthetic solution emulating the spent rinse baths generated in the cyanide-free brass electrodeposition was treated by electrodialysis operated in galvanostatic mode at current levels below and above the limiting current density [11]. One of the principal concerns identified from the previous works was the formation of precipitates at the membrane surface and the degradation of the membrane properties after long-term use. Thus, to ensure the sustainability of the overall process, an optimum strategy regarding membrane cleaning and maintenance is needed.

After long-term ED operations, cleaning the membranes is crucial to restore their features and to extend their lifespan. Fouling, scaling and membrane degradation result

in an increase of the electrical resistance and a decrease of the membrane permselectivity [12–14]. In general, authors use some well-known protocols to study the influence of artificial ageing on various membrane properties [15,16]. García-Vasquez et al. evaluated the effects of acidic and alkaline cleanings on the properties of homogeneous and heterogeneous anion-exchange membranes; they identified that, in the case of heterogeneous anion-exchange membranes, the membrane structure is more resistant against alkaline conditions, while it undergoes severe degradation after cleaning with strong acidic solutions [17]. In their study, the membranes were aged via soaking in concentrated HCl and NaOH solutions. However, to our knowledge, studies investigating the cleaning of ion exchange membranes after long-term electrodialysis treatments involving the application of current and, consequently, the passage of metallic species through the membrane structure is scarce. Especially interesting is the case of fouling involving complex species that are present in effluents coming from hydrometallurgical processes. The concentration of the cleaning agents is another factor that is commonly overlooked.

In this work, we investigate the effects of a three-stage chemical cleaning on the performance recovery and the structure integrity of ion-exchange membranes used in the treatment of synthetic wastewaters emulating spent cyanide-free brass electroplating baths. An alkaline cleaning procedure with solutions of 0.1, 0.5 and 1.0 $mol \cdot L^{-1}$ NaOH was tested for the used anion- (AEM) and cation-exchange membranes (CEM), following an order of increasing concentrations. The chemical cleaning efficiency in terms of membrane electrochemical performance was checked after each stage by conducting chronopotentiometric measurements, from which the dynamic response of the membranes was monitored. The steady-state behavior of the membrane systems was also evaluated from current-voltage curves (CVC), from which the evolution of important membrane properties such as the limiting current density (i_{lim}), the ohmic resistance (R_1) and the overlimiting resistance (R_3) was assessed. After the complete three-stage cleaning, the presence of foulants and the stability of the structure was also evaluated via FTIR-ATR and SEM/EDS analyses.

2. Materials and methods

2.1.Electrodialysis

The membranes used in the present investigation were subject of a prior study, which involved the conduction of chronopotentiometric measurements and use of the membranes in an electrodialysis process [11]. The electrodialysis test was carried out in a five-compartment cell over 344 h, where 4 L of a synthetic wastewater emulating the composition of effluents generated in the brass electroplating industry were treated. Two membrane pairs, consisting each of a cation-exchange membrane (HDX100) and an anion-exchange membrane (HDX200), separated the five compartments of the electrodialysis setup. The membranes had an active area of 16 cm^2. Electrodes made of titanium coated with ruthenium and titanium oxides ($70RuO_2/30TiO_2$) were used as cathode and anode. The applied current density was 1.2 $mA \cdot cm^{-2}$, which corresponds to 70% of the limiting current density of the membranes/electrolyte system. This limiting current density was determined prior to the electrodialysis operation, by registering current- voltage curves for the cation- and anion-exchange membranes in the electrodialysis cell filled with the synthetic wastewater. For this, platinum wires were placed at the interfaces of the AEM and CEM facing the solutions to be diluted and concentrated in ED. Voltmeters were connected directly to the platinum wires to measure the potential drop across both membranes when successive current densities were applied to register the current-voltage curves. The i_{lim} of the membranes in the electrodialysis system was determined from the obtained CVCs using the same methodology employed for determining limiting current densities in the chronopotentiometric evaluations, as will be presented in detail in Section 2.6.

After the 344 h of electrodialysis operation, the ion-exchange membranes were evaluated, by chronopotentiometry, and cleaned using the procedure described in Section 2.4; their properties were reevaluated according to the methods described in Sections 2.5, 2.6 and 2.7.

2.2.Working solution

The working solution used in the chronopotentiometric tests after each cleaning step was the same solution previously treated by electrodialysis. The solution was prepared

using $CuSO_4 \cdot 5H_2O$, $ZnSO_4 \cdot 7H_2O$, EDTA disodium salt and NaOH as reagents. The composition of the working solution resembles that of the rinse effluents generated in the cyanide-free brass electroplating of metallic pieces [9]. Table 1 presents the initial composition of the working solution used in the present study, along with its pH and conductivity.

Table 1 - Initial composition of the working solution of the chronopotentiometric tests.

Molar concentration ($mol \cdot L^{-1}$)				pH	Conductivity ($mS \cdot cm^{-1}$)
$CuSO_4 \cdot 5H_2O$	$ZnSO_4 \cdot 7H_2O$	EDTA	NaOH		
0.0006	0.0014	0.0015	0.03	12.25	5.3

2.3.Ion-exchange membranes

The anion- and cation-exchange membranes evaluated in the present study are the commercial HDX200 and HDX100 membranes, respectively. Both were supplied by Hidrodex. The membranes have a heterogeneous structure with reinforcing fabrics at both surfaces to enhance their mechanical resistance. The HDX200 presents quaternary amine as fixed groups, whereas the HDX100 presents sulfonic acid functional groups. The characteristics of both membranes are presented in Table 2.

Table 2 - Main characteristics of HDX 100 and HDX 200 membranes provided by the supplier.

Parameter	HDX100	HDX200	Unit
Ion group attached	$-SO_3^-$	$-NR_3^+$	–
Water content	35–50	30–45	%
Ion exchange capacity	≥2.0	≥1.8	$mol \cdot kg^{-1}$ (dry)
Surface resistance (measured in 0.1 $mol \cdot L^{-1}$ NaCl)	≤20	≤20	$Ohm \cdot cm^2$
Permeselectivity (0.1 $mol \cdot L^{-1}$ KCl/0.2 $mol \cdot L^{-1}$ KCl)	≥90	≥89	%
Burst strength	≥06	≥0.6	MPa
Dimensional change rate	≤2	≤2	%
Water permeability	≤0.1 (< 0.2 MPa)	≤0.2 (< 0.035 MPa)	$mL \cdot h \cdot cm^{-2}$

2.4.Cleaning procedure

After the electrodialysis and chronopotentiometric tests performed in our previous work [11], the membranes were forwarded to the three-stage cleaning procedure, which is described as follows:

1. Both cation- and anion-exchange membranes used in the electrodialysis operation were rinsed with distilled water and immersed in the cleaning solution of NaOH (0.1 mol·L^{-1}) for 72 h.
2. Then, the membranes were rinsed with water for 24 h to remove any trace of the cleaning solution, immersed in the working solution (brass electrodeposition synthetic rinse effluent – Table 1) for 24 h and analyzed via chronopotentiometry. Ion transport through the membranes in the state reached after the first chemical cleaning was evaluated from the chronopotentiometric and current-voltage curves.
3. The membranes were rinsed, and the cleaning procedure was repeated twice, for 72 h in each cleaning stage, using higher concentrations of the NaOH cleaning solutions (0.5 mol·L^{-1} and 1.0 mol·L^{-1}). After each cleaning stage, ion transport through the membranes was analyzed again by means of chronopotentiometry, using the working solution described in Table 1. The cleaned membranes were also analyzed by means of FTIR-ATR and SEM/ EDS in order to find possible alterations in their structure.

The chronopotentiometric results obtained after each cleaning step were compared with the results obtained after the electrodialysis process (before the cleaning procedure) and with those obtained with the virgin membranes. The FTIR-ATR and SEM/EDS results were also compared with those obtained with the virgin membranes. For a better understanding of the cleaning and chronopotentiometric steps, the procedure is detailed in Fig. 1.

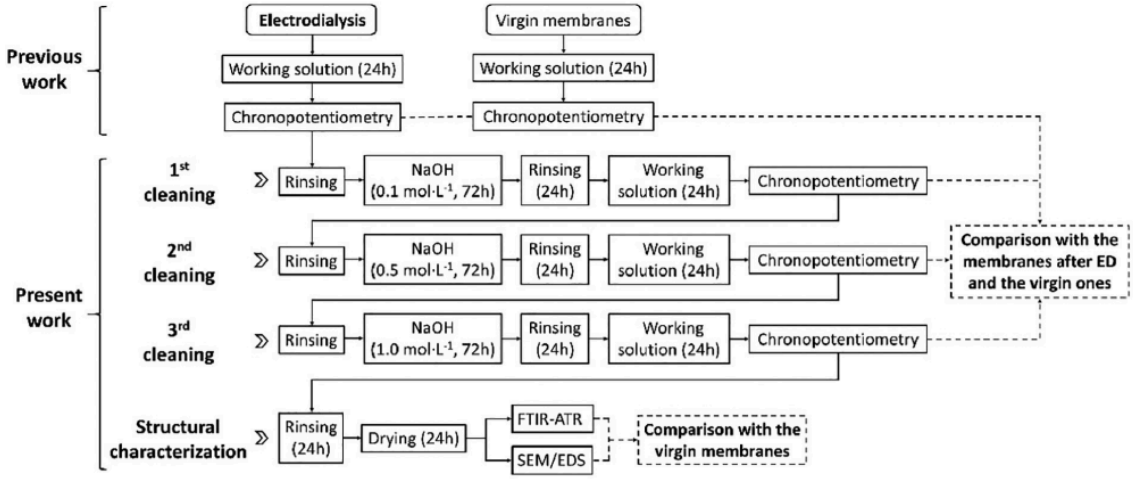

Figure 1 - Cleaning and chronopotentiometric procedures performed after electrodialysis.

2.5.Chronopotentiometric measurements

Chronopotentiometric tests were conducted using a three-compartment reactor with a cation- and an anion-exchange membrane that separated the central compartment from the cathode and anode, respectively. Two graphite bars were used as electrodes and were connected to a potentiostat/galvanostat (Autolab, PGSTAT 20). Two Ag/AgCl reference electrodes immersed into two Luggin capillaries were installed at each side of the membranes under study, to measure the evolution of the potential drop of the membrane/electrolyte system over time. All tests were conducted in duplicate, at room temperature and without stirring. The estimated relative error between the values of the transport properties (see Section 2.6) was below 5%.

For the chronopotentiometric measurements, current pulses at different values of constant current were applied for 300 s. During the application of a constant current density, cations move towards the cathodic compartment and anions towards the anodic one, while the membranes act as selective barriers allowing the transport of their respective counter-ions and impeding the transport of their respective coions. As a consequence of the membrane selective transport, concentration gradients are formed in the diffusion boundary layers adjacent to the membranes' surface. Therefore, the potential drop measured between the reference electrodes can be considered as an indicator of the progress of concentration polarization taking place in the system. In addition to this, the initial potential drop registered in each chronopotentiogram after switching on the current can be considered as a measure of the system's ohmic resistance, including that related to the membrane structure. Once the current is switched off, concentration profiles generated in each diffusion boundary layer dissipate and the bulk solution concentration is reestablished along the electrolyte compartments during the relaxation of the system. This process is registered during 100 additional seconds before the application of the next pulse. For each membrane system, several chronopotentiograms were registered by applying successive current pulses at increasing values of current density. A schematic representation of the chronopotentiometric system can be found elsewhere [18].

2.6. Determination of transport properties

Current-voltage curves were obtained by plotting the steady state value of the potential drop registered in each chronopotentiogram against the corresponding value of

applied current density. The transport properties of the membranes/electrolyte system were determined from the current–voltage curves. A typical current-voltage curve consists of three differentiated regions:

(a) an initial region of quasi-ohmic behavior at low values of current density, where current and voltage follow a linear relationship,
(b) a second region where the so-called limiting current density (i_{lim}) is reached and the curve flattens, showcasing an abrupt increase in the system's resistance because the electrolyte concentration approaches zero next to the depleting membrane surface; and
(c) a third region of overlimiting current transfer ($i > i_{lim}$), where ion supply to the membrane surface is again activated and current density rises again with the transmembrane voltage.

Typical curves including the three regions of membrane-electrolyte behavior were obtained in the present work (as shown in Fig. 2). Limiting current densities (i_{lim}) were determined from the intersection of the tangential lines of the first and second regions of the CVC. The ohmic resistances (R_1) were calculated as the inverse of the slope (α_1) of the tangential line of the first region of the CVC (ohmic region), and the electrical resistance of the overlimiting region (R_3) was calculated similarly to the ohmic one, i.e., from the inverse of the slope (α_3) corresponding to the overlimiting region of the CVC.

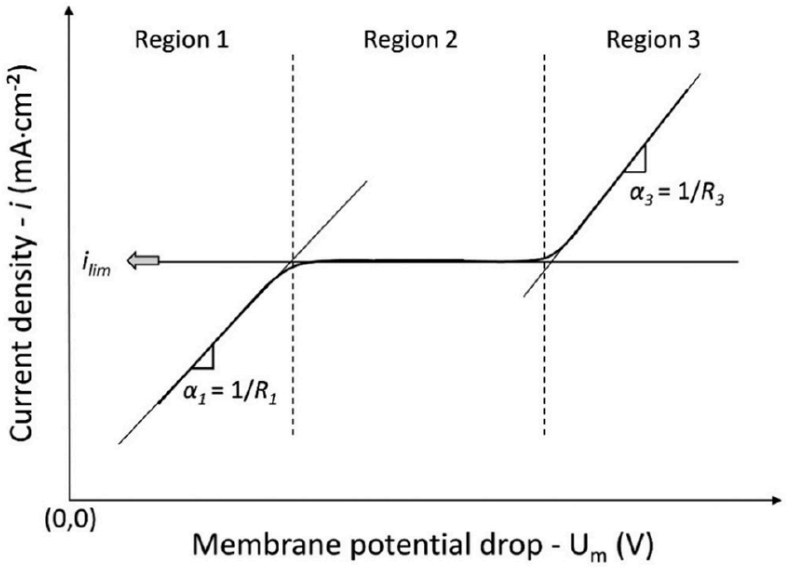

Fig. 2. Representation of a typical current-voltage curve.

3. Results and Discussion

The alkaline cleaning procedure was evaluated for the anion- and cation-exchange membranes used in electrodialysis. After each cleaning step (with 0.1, 0.5 and 1.0 mol·L^{-1} NaOH solutions), chronopotentiograms and current-voltage curves were registered and analyzed.

3.1. Evaluation of current-voltage curves

The current-voltage curves obtained after the electrodialysis process and after each cleaning step are shown in Fig. 3, whereas the limiting current densities, ohmic resistances and overlimiting resistances determined from the curves are shown in Table 3. The results obtained for the virgin membranes, without being exposed to electrodialysis or to the cleaning procedure, are also shown. Note that the shapes of the curves obtained with the virgin membranes are considerably different from those obtained with the membranes after being used in the electrodialysis and after the subsequent cleaning procedures. This evolution in the membrane response suggests structural changes happening in the membranes as a consequence of their use. The changes in membrane behavior entail a change in their transport properties, as shown below.

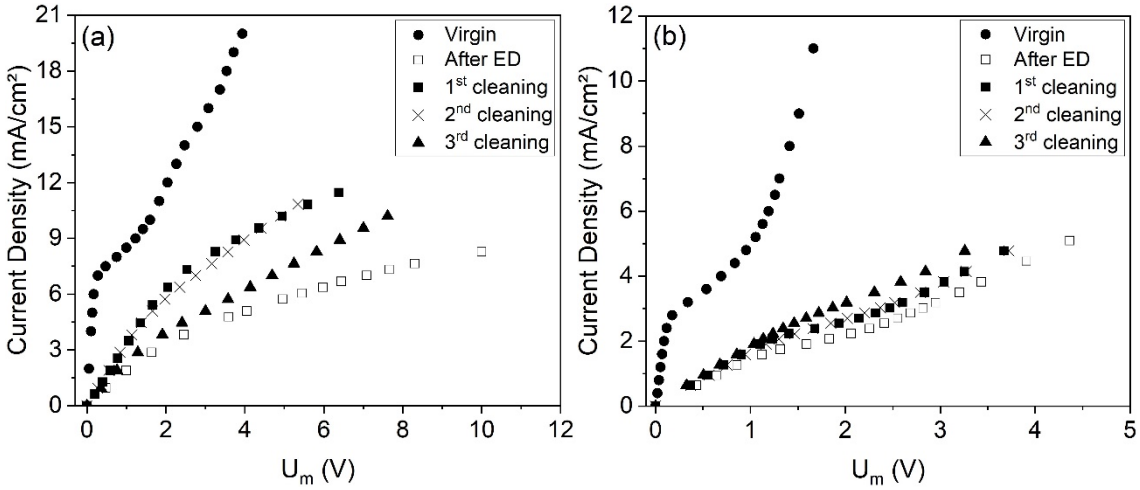

Figure 3 - Current-voltage curves of the a) AEM and b) CEM after electrodialysis and after the 1st, 2nd and 3rd cleaning steps, besides the virgin membranes.

Table 3 - Limiting current density and electrical resistances (R_1 and R_3) of both ion-exchange membranes after electrodialysis and the cleaning steps.

	Anion-exchange membrane			Cation-exchange membrane		
	i_{lim} (mA·cm^{-2})	R_1 (Ω·cm^2)	R_3 (Ω·cm^2)	i_{lim} (mA·cm^{-2})	R_1 (Ω·cm^2)	R_3 (Ω·cm^2)
Virgin	6.9	28	189	2.7	44	89
After electrodialysis	3.7	572	2333	1.6	672	734
1st cleaning	6.8	305	1060	2.1	582	659
2nd cleaning	5.4	298	720	1.9	591	730
3rd cleaning	3.2	398	941	2.4	549	746

According to Fig. 3 and Table 3, the first cleaning (0.1 mol NaOH·L^{-1}) seems to be the most suitable to recover the original features of the anion-exchange membrane. After the first cleaning, the i_{lim} increased by 84% in relation to its value after electrodialysis, whereas the ohmic and overlimiting resistances decreased by 47% and 55%, respectively. Despite the decrease in R_3 of the AEM (69%) after the 2nd cleaning (0.5 mol NaOH·L^{-1}), R_1 did not change significantly. Moreover, the 2nd cleaning caused a decrease in i_{lim}, which was not expected. This may have occurred due to the degradation of the AEM, since all chronopotentiometric tests were conducted using the same electrolyte. This will be discussed in detail below.

The 3rd cleaning (1.0 mol NaOH·L^{-1}) caused an inversion in the behavior of the properties of the AEM: a great increase in R_1 and R_3 occurred, if compared to the 2nd cleaning; and a decrease in the limiting current density was observed. This may have also occurred due to the degradation of the AEM. Sata et al. [19] showed that AEMs deteriorate from three parts: the mechanical support (backing fabric), the polymer matrix, and the anion-exchange groups fixed on it. Besides, Merle et al. [20] verified that quaternary ammonium sites, present in the HDX200 membrane, are unstable under alkaline conditions and can be degraded following two main pathways: elimination and/or nucleophilic substitution [21]. Hence, the degradation of the AEM by the 1 mol·L^{-1} NaOH solution may have reduced its fraction of conductive area (ε), which will be confirmed by SEM/EDS. This caused the decrease in the limiting current density after the 2nd and, mainly, the 3rd cleaning step.

The increase in R_1 of the AEM after the 3rd cleaning (in relation to the 2nd one) supports the suggestion regarding the decrease of ε, since the increase in the inhomogeneity contributes to increase the membrane resistance due to the more tortuous counter-ion pathway [18]. In other words, a loss of ion conducting sites entails a decreased connectivity between ion-exchange sites in the membrane matrix, resulting in longer effective distances to be crossed by the current carriers. Besides, the degradation

of the quaternary ammonium sites reduces the attraction between membrane and ions, which also increased the ohmic resistance [22].

The increase in R_3 of the AEM after the 3rd cleaning (in relation to the 2nd one) is also in agreement with the reduction of ε, since Choi and Moon [23] verified that the conversion of quaternary amines into their tertiary and neutral forms leads to an increase in the plateau length. As this property represents the energy required to disrupt the diffusion boundary layer involving a change of the main mass transfer mechanism from diffusion and migration to electroconvection [24], the increase in plateau length denotes a hindered onset of overlimiting phenomena. Therefore, the overlimiting resistance, R_3, increased when the inhomogeneity degree of the membrane increased. Similar results were obtained by Ibanez et al. [25].

Concerning the cation-exchange membrane, the cleaning steps led to similar results on the ohmic resistance. The overlimiting resistances did not show significant differences, except after the 1st cleaning, where the lowest R_3 value was obtained. The i_{lim} increased after the 1st cleaning compared to its value after electrodialysis, remained practically constant after the 2nd cleaning, and increased again after the 3rd one. Although the 3rd cleaning was the most efficient to recover the i_{lim} and the ohmic resistance to their initial values observed with the virgin membrane, the application of this third cleaning stage is not recommended, since the 1st cleaning showed similar results and should be less harmful for the membrane chemical structure.

The differences between the values of transport properties after each cleaning are less evident for the CEM than for the AEM; this occurred since anion-exchange membranes are more susceptible to degradation than cation-exchange ones [26]. Hence, the NaOH solutions were not able to degrade the CEM so intensively as the AEM. These results are discussed further in the FTIR-ATR and SEM/EDS evaluations.

3.2. Evaluation of the chronopotentiograms

Chronopotentiograms were registered for evaluating the influence of each cleaning step on the concentration polarization and the tendency of precipitates formation. The potential drop shown in the chronopotentiograms is the total one (measured). Hence, it also shows the influence of the cleaning procedure on the ohmic resistance of the system and provides a global measure of the membranes' performance in electrodialysis operations. Differently, some authors represent the “reduced potential drop” by excluding

the ohmic potential drop for comparing different membranes [27]. In our article, we would like to emphasize that, the ohmic potential drop can also be significantly altered by changes in the membrane structure, such as those resulting from a reduction in the fraction of conducting regions.

3.2.1. Chronopotentiograms of the anion-exchange membrane

Chronopotentiograms of the anion-exchange membrane under three applied current densities after each cleaning step are presented in Fig. 4.

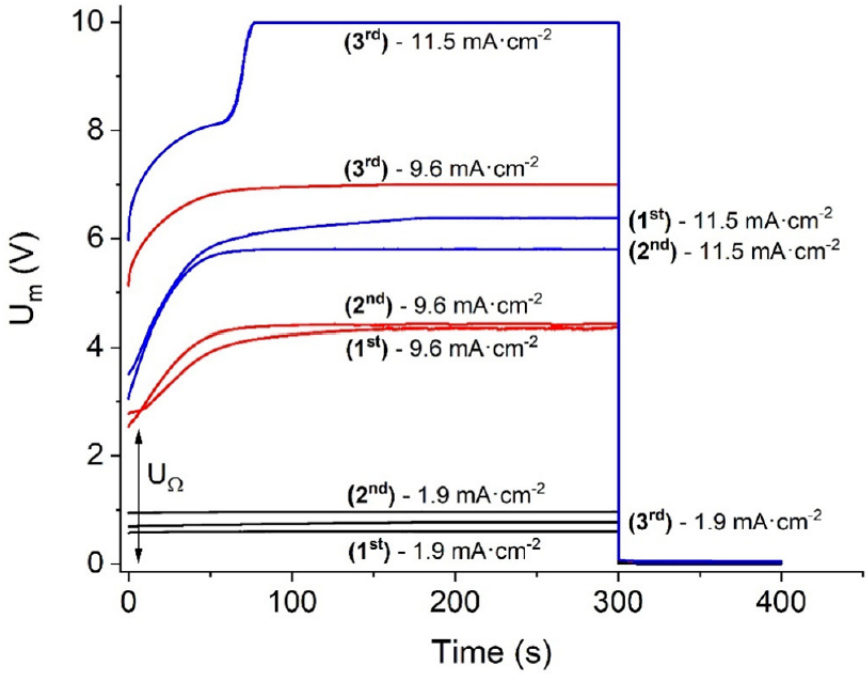

Figure 4. Chronopotentiograms for the anion-exchange membrane after each cleaning step (1st, 2nd, 3rd). Each color represents an applied current density.

For the AEM, interesting behaviors have been verified with the increase in the current density. Under 1.9 mA·cm^{-2}, the curves showed a constant behavior over time, without inflection points. Therefore, under this condition, migration and diffusion are the main mass transfer mechanisms.

Under application of current densities above the limiting one, an inflection point related to the occurrence of intense concentration polarization can be noted. For 9.6 mA·cm^{-2}, the curves obtained after the 1st and 2nd cleaning steps are very close to each other, especially at the steady-state condition. However, the curve registered after the 3rd cleaning under 9.6 mA·cm^{-2} is quite distant from the others and presents a greater value of potential drop. The same behavior can be seen for 11.5 mA·cm^{-2}; the final potential drop of the curve obtained after the 1st cleaning is similar to that obtained after the 2nd one

(values of U_m around 6 V), whereas the final potential drop of the curve registered after the 3rd cleaning is considerably higher than the others. This occurred, in part, because of the greater jump in potential drop at the beginning of the chronopotentiogram of the 3rd cleaning. This initial jump, registered immediately when the current is switched on, is related to the ohmic potential drop (U_Ω - shown in Fig. 4) over the membrane and two adjacent solutions, where the concentrations are not yet affected by concentration polarization [27,28]. The greater U_Ω value after the 3rd cleaning indicates an increase in the resistance of the non-polarized DBL [29] and, consequently, in the overall cell voltage. This may be related to the degradation of the membrane, as suggested by the current-voltage curves. In electrodialysis, the ohmic drop must be minimized, since energy inputs and electricity costs are directly affected by the cell voltage [8].

Another feature can be seen in the chronopotentiograms: an unexpected and very sharp increase in the potential drop in the curve of the 3rd cleaning under application of 11.5 $mA \cdot cm^{-2}$ and the achievement of the maximum potential drop supported by the potentiostat/galvanostat (10 V). This is a typical response observed when precipitate formation takes place on the surface of the membrane or inside it [30]. Since all the chronopotentiograms were registered using the same electrolyte (Table 1), this behavior supports the suggestion of the membrane degradation by the NaOH in 1.0 $mol \cdot L^{-1}$. As mentioned previously, quaternary amines are unstable at alkaline pH values and can be converted into tertiary ones, which have higher catalytic activity towards water dissociation than the quaternary amines [17,31]. Hence, the 3rd cleaning may have led to the decrease of quaternary ammonium groups in favor of tertiary amines [32,33] and, during chronopotentiometry, intense water dissociation may have occurred at the AEM. This led to the intense migration of hydroxyl ions through the membrane, whereas protons accumulated on its cathodic side, causing a pH decrease. According to the speciation diagram constructed with the composition of the working solution of electrodialysis (Fig. 5), CuO is present in the initial state of the solution (pH 12.25) and under lower pH values. Hence, this insoluble species may have been responsible for the non-expected increase in the potential drop after the 3rd cleaning. These results indicate that the cleaning step with 1.0 $mol \cdot L^{-1}$ NaOH is not recommended for the anion-exchange membrane.

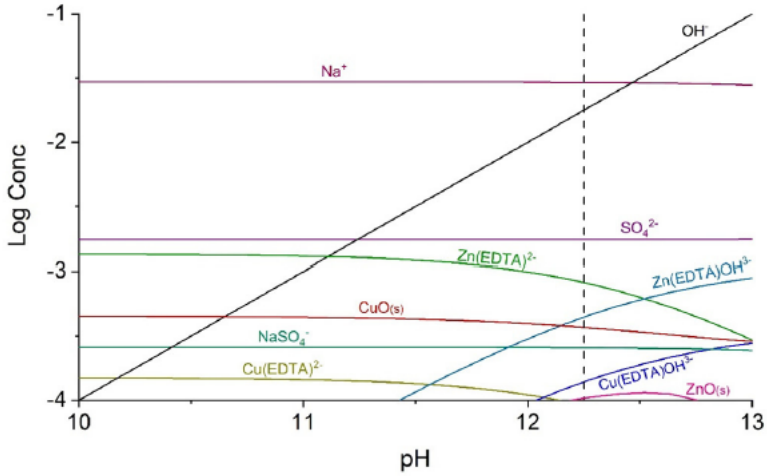

Figure 5. Speciation diagram constructed with the composition of the working solution. The dashed line indicates the initial solution pH (12.25).

3.2.2. Chronopotentiograms of the cation-exchange membrane

Fig. 6 shows chronopotentiograms obtained for the cation-exchange membrane after each cleaning step.

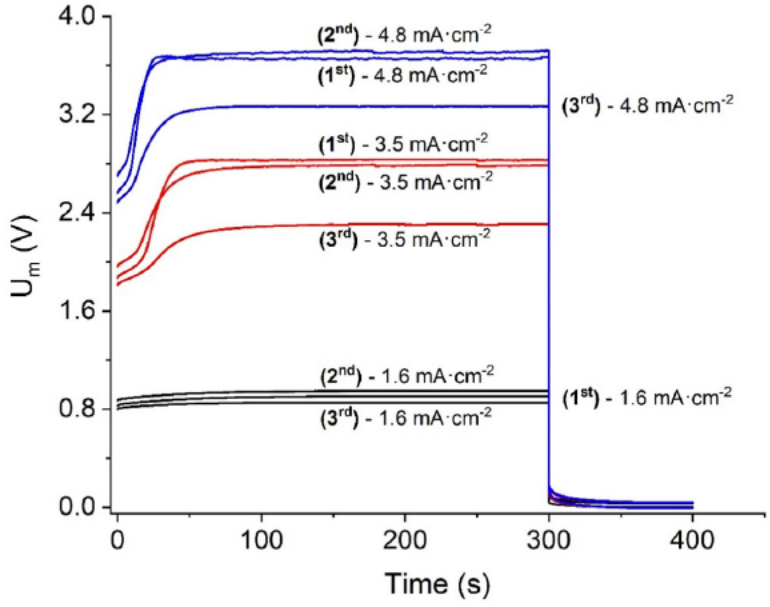

Figure 6. Chronopotentiograms for the cation-exchange membrane after each cleaning step (1st, 2nd, 3rd). Each color represents an applied current density.

Under application of 1.6 mA·cm^{-2} ($i < i_{lim}$), migration and diffusion control ion transfer since the membrane system is in underlimiting condition, i.e., intense concentration polarization did not occur. Under current densities above the limiting one (3.5 and 4.8 mA·cm^{-2}), the behavior of the curves of the 1st and 2nd cleaning steps are

very similar, as well as their values of final potential drop. However, lower values of potential drop were obtained after the 3rd cleaning. The same trend was verified for the U_{Ω} values. These results are in accordance with the R_1 values presented in Table 3, which were calculated from the slope of the CVCs.

For the cation-exchange membranes, atypical behaviors, such as an unexpected increase in potential drop, were not verified in the chronopotentiograms. As mentioned, anion-exchange membranes are more susceptible to degradation than cation-exchange ones. Besides, anionexchange membranes are more susceptible to the occurrence of water dissociation than the cation-exchange ones [23], which also explains the absence of precipitates on its surface during chronopotentiometry.

3.3. FTIR-ATR analysis

A FTIR-ATR analysis was performed for evaluating the modifications on the AEM and CEM structure after the cleaning procedure. Both membranes exhibit modifications on their spectral profile after electrodialysis and the cleaning procedure, especially in the frequency region between 1750 and 750 cm^{-1}.

3.3.1. Anion-exchange membrane

Fig. 7 presents the infrared spectra for the virgin and cleaned anion-exchange membranes after the electrodialysis test.

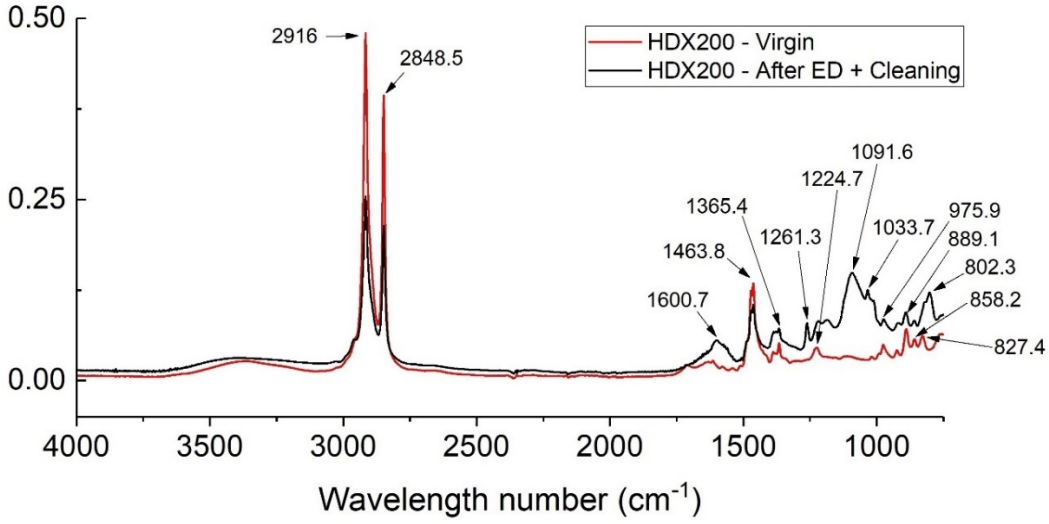

Figure 7. IR spectra of the virgin anion-exchange membrane and after 344 hours of electrodialysis + three cleaning steps.

In Fig. 7, the peaks at 2916 and 2848.5 cm^{-1} correspond to $\nu_{as,s}CH_2$, respectively [33], where indexes “as” and “s” refer to asymmetric and symmetric vibrations, respectively. Both peaks are present in the used AEM with lower intensity, which means that it could have been degraded by electrodialysis or by the cleaning procedure.

A new peak at 1600.7 cm^{-1} appeared after the membrane use and, as showed by Kołodyńska et al. [34], this may be due to the presence of $[Cu(EDTA)]^{2-}$. Besides, Sawyer and Mckinnie [35] found a peak at 1605 cm^{-1} that corresponds to the $-COO^-$ present in the complex formed by EDTA and copper ions. Hence, this indicates that the cleaning procedure was not able to completely remove these species from the anion-exchange membrane or that these ions were deposited on the membrane surface after the last chronopotentiometric evaluation.

The peaks at 1463.8 and 1365.4 cm^{-1} are present in both spectra and are related to the $-CH_2-$ [33,36,37]. A decrease in the intensity of the peak at 1463.8 cm^{-1} can be noted after the membrane use, which occurred due to its degradation. Conversely, the intensity of the peak at 1365.4 cm^{-1} increased. This may be a consequence of the presence of a species composed of EDTA. In line with our results, Esteban et al. [38] found a band assigned to $N-H^+$ deformation at 1364 cm^{-1} in the solid sample of EDTA disodium salt.

From 1365.4 to 750 cm^{-1}, all the bands showed higher intensity after the membrane use, which may be attributed to fouling occurrence. At 1261.3 cm^{-1}, a new band was observed. In general, this peak is attributed to the C-O [39] or C-N stretching vibrations [40]. However, this may also be related to the deposition of any species with EDTA, since Lanigan and Pidsosny [41] evaluated a sample of EDTA and found a peak at 1262 cm^{-1} related to $-COO^-$. At 1224.7 cm^{-1}, there is a peak for both anion-exchange membranes and this corresponds to the N-C stretching vibrations from the quaternary ammonium functional sites [42].

A peak is present at 1091.6 cm^{-1} only for the used membrane. Lanigan and Pidsosny [41] found a peak at 1109 cm^{-1} associated with the Cu-EDTA complex. Besides, the authors verified that the complexation of EDTA with Cu^{2+} or Zn^{2+} leads to a shift in the bands, and the shift degree depends on the ionic or covalent character of the complex formed. As the peak obtained at 1091.6 cm^{-1} is close to that found by Lanigan and Pidsosny [41] (1109 cm^{-1}), the appearance of this band may be a consequence of the formation of a complex of EDTA with copper or zinc ions. Besides, the results from Esteban et al. [38] support this suggestion, since they found a peak at 1090 cm^{-1}, which corresponds to the C-N asymmetric stretching of an EDTA disodium salt sample.

At 1033.7 cm^{-1} the band is present in the virgin membrane and in the used one, but its intensity is greater in the latter. For the virgin membrane, this peak is related to the ν(N-C) stretching vibrations from the quaternary ammonium functional sites [43], whereas for the used one, this is also related to the fouling occurrence. Lanigan and Pidsosny [41] found a peak at 1020 cm^{-1} related to the δOH(COOH) present in a sample of EDTA disodium salt. Sawyer and Mckinnie [35] found a peak at 1025 cm^{-1} that corresponds to the -COO- of the complex of EDTA with copper ions. Hence, the greater intensity of the band at 1033.7 cm^{-1} in the used membrane may be due to a complex with metals and EDTA, besides the ν(N-C) stretching vibrations from the quaternary ammonium.

The bands at 975.9, 889.1 and 858.2 cm^{-1} are present in both AEMs and are associated with the C-H presence [34,44,45]. The peak at 827.4 cm^{-1} also corresponds to the C-H and is present only in the virgin membrane, which suggests its degradation after its use. Lastly, the peak at 802.3 cm^{-1}, in general, is also related to the C-H, but as it is present only in the used membrane, this may be related to the deposition of insoluble species or metal complexes.

3.3.2. Cation-exchange membrane

The infrared spectra for the virgin and cleaned cation-exchange membrane after electrodialysis is shown in Fig. 8.

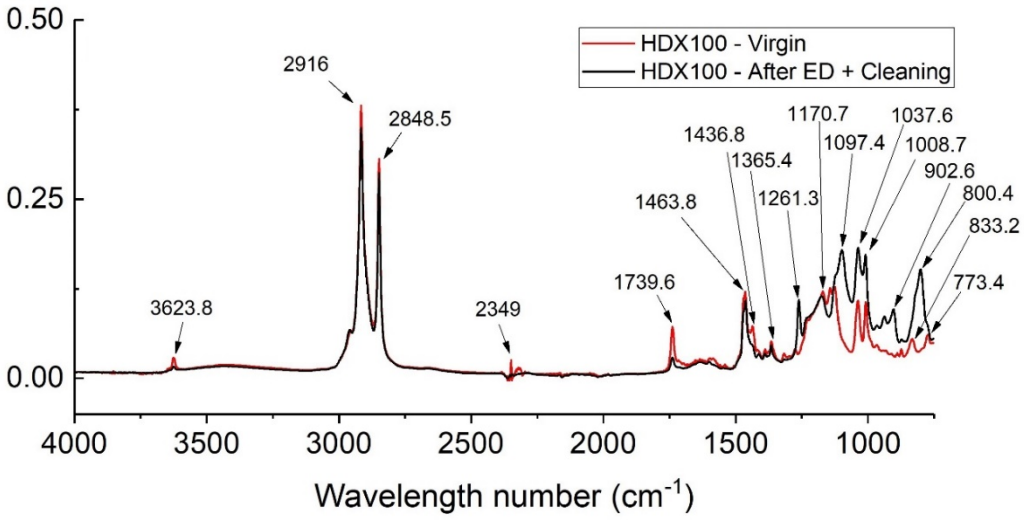

Figure 8. IR spectra of the virgin cation-exchange membrane and after 344 hours of electrodialysis + three cleaning steps.

The peak at 3623.8 cm^{-1} corresponds to the OH stretching [46] and is present only in the virgin membrane, since it was degraded after being used. The bands at 2916 cm^{-1} and 2848.5 cm^{-1} correspond to the $\nu_{as,s}CH_2$, respectively [33]. For the CEM, these peaks did not show lower intensities after the membrane usage, as verified for the AEM. This may be explained by the lower degradation of the CEM than the AEM due to the different species that crossed each membrane. Besides, the higher degradation of the fixed groups of the AEM may be a consequence of the current induced membrane discharge (CIMD) effect. In this case, the hydroxyl ions may have caused the decomposition of the quaternary groups [23,47], and this phenomenon does not occur at CEMs. These results are in accordance with the chronopotentiometric curves shown in Section 3.2.

The peak at 2349 cm^{-1} is related to the CO_2 present in the air [40]. The band at 1739.6 cm^{-1} corresponds to the C=O stretching [48,49] and for the used membrane, a decrease in its intensity was verified. Both CEMs showed a peak related to the bending of -CH_2- at 1463.8 cm^{-1}, whereas only the virgin membrane presented a peak related to the CH_2 group at 1436.8 cm^{-1} [36,42]. A peak at 1365.4 cm^{-1} was observed for both membranes and this corresponds to δC-H [37].

The first peak that appeared only for the used CEM can be seen at 1261.3 cm^{-1}. Sawyer and Mckinnie [35] found a peak at 1260 cm^{-1}, which was associated with the -COO- group or C-N bond present in a sample of EDTA disodium salt. Besides, the authors found a peak at 1255 cm−1 that was related to the -COO− group present in a Cu-EDTA complex. Hence, the peak at 1261.3 cm^{-1} found in the present work suggests fouling/scaling occurrence.

At 1170.7 cm^{-1}, a peak that corresponds to the $–SO_3$ – functional groups was verified for the virgin and used CEM with the same intensity. At 1097.4 cm^{-1}, another band was obtained only for the used membrane, which also suggests fouling/scaling. Sawyer and Mckinnie [35] found a peak at 1110 cm^{-1} associated with the C-N present in a complex of Zn-EDTA and a peak at 1120 cm^{-1} related to the C-N present in a sample of EDTA disodium salt. As discussed for the AEM in Section 3.3.1, the complexation of EDTA with Cu^{2+} or Zn^{2+} ions leads to a shift in the bands, and the shift degree depends on the ionic or covalent character of the complex formed [41]. Hence, the peak at 1170.7 cm^{-1} may be related to any insoluble species, probably with EDTA.

The bands at 1037.6 cm^{-1} and 1008.7 cm^{-1} correspond to the $–SO_3$ functional groups [42,44] and are present in the spectra of both CEMs, but with higher intensity for the used membrane. These peaks may be related to the fouling/scaling occurrence, since

Wang et al. [50] found a peak at 1043 cm^{-1} assigned to the ν_{as}(C-N) present in a sample of EDTA, whereas Lanigan and Pidsosny [41] found a peak at 1008 cm^{-1} assigned to νC-C(CH_2COOH). The peaks at 902.6 cm^{-1} and 800.4 cm^{-1} are present only in the used CEM, which may be also associated with the agglomeration of complex species with EDTA. This is supported by the work of Lanigan and Pidsosny [41], since they found a peak at 915 cm^{-1} related to the νC-C(CH2COO−) present in a sample of EDTA disodium salt.

Finally, the bands at 833.2 cm^{-1} and 773.4 cm^{-1} are present only in the spectra of the virgin CEM, indicating its degradation after its use. Both peaks correspond to the C-H bending [51–53]. In general, the AEM showed more peaks related to degradation and fouling occurrence than the CEM, which is in accordance with the results from chronopotentiometry.

3.4. SEM/EDS analysis

Scanning electron microscopy (SEM) analysis was conducted after the cleaning procedure for evaluating modifications in the structure of the anion- and cation-exchange membranes. Energy dispersive spectroscopy (EDS) analysis was also performed through point scan for qualitatively characterizing the samples. The SEM images are present in Fig. 9 for the anion-exchange membrane HDX200 and in Fig. 10 for the cation-exchange membrane HDX100.

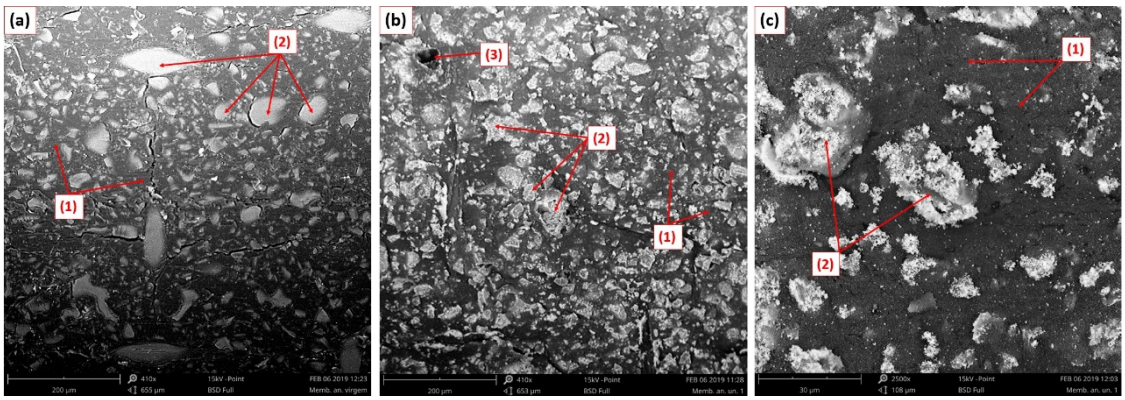

Figure 9. SEM images of the a) virgin anion-exchange membrane HDX200 (655 µm) and after 344 h of electrodialysis + three cleaning steps at b) 653 µm and c) 108 µm.

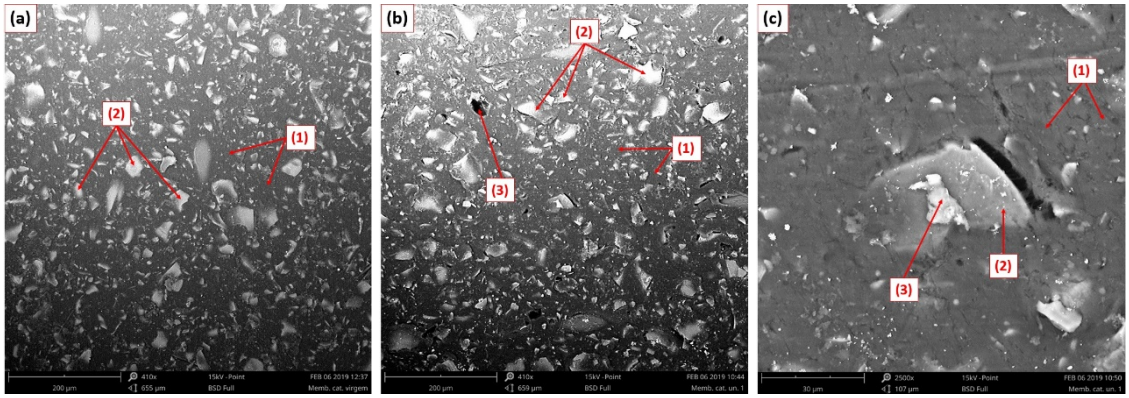

Figure 10. SEM images of the a) virgin cation-exchange membrane HDX100 (655 µm) and after 344 h of electrodialysis + three cleaning steps at b) 659 µm and c) 107 µm.

Both membranes have their structure characterized by clearly distinct conductive and nonconductive regions, since there are dispersed agglomerates of ion-exchange particles typical of heterogeneous membranes. Nonconductive regions are shown at point 1 of Figs. 9(a,b,c) and 10 (a,b,c), whereas conductive regions with functional groups are presented at point 2 of Figs. 9a and 10a. Point 2 of Figs. 9b and 10b also show conductive regions in the membranes after electrodialysis but, in this case, the EDS analysis showed the presence of some species agglomerated on the fixed charges. The results on EDS analyses are provided in the Supplementary Information.

For the AEM, the species agglomerated can be clearly seen in Fig. 9c (point 2) and are composed mainly of zinc, which may be present as an oxide (ZnO) or complexed with EDTA [$Zn(EDTA)^{2-}$ or $Zn(EDTA)\ OH^{3-}$]. The presence of an agglomerate of zinc at the AEM is a consequence of the inefficiency of the cleaning procedure for removing the scaled/fouled species or due to the last chronopotentiometric test performed after the 3rd cleaning. These results support those presented in the FTIR-ATR analysis.

For the cation-exchange membrane, the agglomeration of species at the fixed charges is shown in Fig. 10c; at point 2, the functional group can be seen, whereas at point 3 an agglomerate of sodium is shown. Sodium was attracted to the fixed charges since the membrane cleaning was conducted with NaOH solutions.

Lastly, the degradation of the polymer structure was also observed; points 3 of Figs. 9b and 10b show some cavities, which appeared because of the exposure of the membranes to the extremely alkaline solutions [54]. These cavities are present exactly on the fixed charges, which means that the concentration of active functional groups was reduced in both membranes. The presence of these cavities finally confirms the results

obtained in the evaluation of current-voltage and chronopotentiometric curves, since a decrease in the fraction of conductive area of the membranes was suggested. Some authors reported that membrane ageing affects the polymeric chains more than the ion-exchange groups, which leads to the loss of permselectivity [55,56]. Hence, the use of 1.0 mol $NaOH \cdot L^{-1}$ solution is not recommended for the cleaning of ion-exchange membranes used in electrodialysis for treating wastewaters from electroplating industries.

4. Conclusions

In this work, we evaluated the effects of a three-stage chemical cleaning on the properties of heterogeneous cation- and anion-exchange membranes previously used in the treatment, by electrodialysis, of synthetic effluents of the electroplating industry. The membranes were used to treat alkaline solutions containing zinc, copper and EDTA, and were cleaned afterwards in successive stages using increasing concentrations of NaOH (0.1 $mol \cdot L^{-1}$, 0.5 $mol \cdot L^{-1}$ and 1.0 $mol \cdot L^{-1}$).

Alterations in the membrane structure and changes in ion transport through the membranes as a result of the chemical cleaning were evaluated by means of chronopotentiometry, FTIR-ATR and SEM/EDS. The electrochemical measurements reveal a general decrease in the performance of both membranes as a consequence of the long-term electrodialysis process: i_{lim} values decrease, while the ohmic resistances increase notoriously. These results demonstrate the relevance of the cleaning strategy to ensure a satisfactory performance over long-term membrane usage.

Regarding the AEM, the 1st cleaning step conducted with mild NaOH solutions (0.1 $mol \cdot L^{-1}$) was the most useful in restoring the initial i_{lim}, since the i_{lim} of the virgin membranes was practically recovered.

The 1st cleaning caused a decrease of the ohmic and overlimiting resistances, which reached values 47% and 55% lower than those of the used membranes, respectively. Nonetheless, the values of R_1 after the cleaning were still far from those obtained with the virgin membranes. Contrariwise, the second (0.5 $mol \cdot L^{-1}$) and mainly the third cleaning step (1.0 $mol \cdot L^{-1}$) caused an increase in the ohmic resistance and a decline in limiting current density. The registration of high values of ohmic potential drop after the 2nd and 3rd cleaning supports the hypothesis that de-activation of ion-exchange sites by the alkaline solutions takes place. Besides, the degradation of quaternary amine groups into tertiary ones may favor water dissociation at the surface of the AEM.

The electrochemical characterization of the CEM after the successive treatments evidence that degradation of this membrane is not of the same magnitude as that observed for the AEM. In this case, the results were similar after cleaning with the three NaOH solutions. Although the values of i_{lim} were substantially recovered after the cleaning with 0.1 mol·L^{-1} NaOH, the decrease in membrane resistance was very slight. These results may reveal that OH^- ions are not able to penetrate into the inner membrane structure and remove internal fouling efficiently, which can be explained by the exclusion of membrane co-ions by the sulfonic groups. Further cleanings with more concentrate solutions do not improve membrane performance and could increase material degradation.

FTIR-ATR spectra showed several peaks related to degradation and fouling/scaling occurrence especially for the AEM. In general, the peaks are related to the deposition of complexes composed of EDTA with copper and zinc ions. Lastly, SEM images and EDS analysis confirmed the degradation of the membranes and agglomeration of metallic species, mainly at the AEM. The presence of cavities on the fixed charges confirmed the reduction of active functional groups of the membranes and, consequently, their fraction of conductive area. The cleaning with mild alkaline solutions (0.1 mol·L^{-1} NaOH) provides the most satisfactory balance between high degree of performance recovery and low risk of membrane degradation.

Acknowledgements

The authors gratefully acknowledge the financial support given by funding agencies CNPq (Process 141346/2016-7) and CAPES (Process 88881.190502/2018-01). This study was financed in part by the Coordenação de Aperfeiçoamento de Pessoal de Nível Superior - Brasil (CAPES) - Finance Code 001.

References

[1] E. Vera, J. Ruales, M. Dornier, J. Sandeaux, R. Sandeaux, G. Pourcelly, Deacidification of clarified passion fruit juice using different configurations of electrodialysis, J. Chem. Technol. Biotechnol. 78 (2003) 918–925, https://doi.org/10.1002/jctb.827.

[2] D. Labbé, M. Araya-Farias, A. Tremblay, L. Bazinet, Electromigration feasibility of green tea catechins, J. Memb. Sci. 254 (2005) 101–109,

https://doi.org/10.1016/j.memsci.2004.10.048.

[3] M.C. Martí-Calatayud, D.C. Buzzi, M. García-Gabaldón, E. Ortega, A.M. Bernardes, J.A.S. Tenório, V. Pérez-Herranz, Sulfuric acid recovery from acid mine drainage by means of electrodialysis, Desalination. 343 (2014) 120–127, https://doi.org/10.1016/j.desal.2013.11.031.

[4] S. Caprarescu, V. Purcar, D.-I. Vaireanu, Separation of copper ions from synthetically prepared electroplating wastewater at different operating conditions using electrodialysis, Sep. Sci. Technol. 47 (2012) 2273–2280, https://doi.org/10.1080/01496395.2012.669444.

[5] H. Strathmann, Ion-exchange membrane processes in water treatment, Sustain. Sci. Eng. Elsevier, 2010, pp. 141–199, https://doi.org/10.1016/S1871-2711(09)00206-2.

[6] T. Scarazzato, K.S. Barros, T. Benvenuti, M.A. Siqueira Rodrigues, D.C. Romano Espinosa, A. Moura Bernardes, V. Pérez-Herranz, Achievements in Electrodialysis Processes for Wastewater and Water Treatment, Elsevier Inc., 2020, https://doi.org/10.1016/B978-0-12-817378-7.00005-7.

[7] L. Marder, E.M. Ortega Navarro, V. Perez-Herranz, A.M. Bernardes, J.Z. Ferreira, Evaluation of transition metals transport properties through a cation Exchange membrane by chronopotentiometry, J. Memb. Sci. 284 (2006) 267–275, https://doi.org/10.1016/j.memsci.2006.07.039.

[8] M. García-Gabaldón, V. Pérez-Herranz, E. Ortega, Evaluation of two ion-exchange membranes for the transport of tin in the presence of hydrochloric acid, J. Memb. Sci. 371 (2011) 65–74, https://doi.org/10.1016/j.memsci.2011.01.015.

[9] K.S. Barros, E.M. Ortega, V. Pérez-Herranz, D.C.R. Espinosa, Evaluation of brass electrodeposition at RDE from cyanide-free bath using EDTA as a complexing agent, J. Electroanal. Chem. (2020), https://doi.org/10.1016/j.jelechem.2020.114129.

[10] K.S. Barros, D.C.R. Espinosa, Chronopotentiometry of an anion-exchange membrane for treating a synthesized free-cyanide effluent from brass electrodeposition with EDTA as chelating agent, Sep. Purif. Technol. 201 (2018) 244–255, https://doi.org/10.1016/j.seppur.2018.03.013.

[11] K.S. Barros, T. Scarazzato, V. Pérez-Herranz, D.C.R. Espinosa, Treatment of cyanidefree wastewater from brass electrodeposition with EDTA by electrodialysis: evaluation of underlimiting and overlimiting operations, Membranes (Basel) 10 (2020) 69, https://doi.org/10.3390/membranes10040069.

[12] T. Scarazzato, Z. Panossian, J.A.S. Tenório, V. Pérez-Herranz, D.C.R. Espinosa, Water reclamation and chemicals recovery from a novel cyanide-free copper plating bath using electrodialysis membrane process, Desalination. 436 (2018) 114–124, https://doi.org/10.1016/j.desal.2018.01.005.

[13] S. Mikhaylin, L. Bazinet, Fouling on ion-exchange membranes: classification, characterization and strategies of prevention and control, Adv. Colloid Interf. Sci. 229 (2016) 34–56, https://doi.org/10.1016/j.cis.2015.12.006.

[14] K.S. Barros, T. Scarazzato, D.C.R. Espinosa, Evaluation of the effect of the solution concentration and membrane morphology on the transport properties of Cu(II) through two monopolar cation–exchange membranes, Sep. Purif. Technol. 193 (2018) 184–192, https://doi.org/10.1016/j.seppur.2017.10.067.

[15] R. Ghalloussi, L. Chaabane, C. Larchet, L. Dammak, D. Grande, Structural and physicochemical investigation of ageing of ion-exchange membranes in electrodialysis for food industry, Sep. Purif. Technol. 123 (2014) 229–234, https://doi.org/10.1016/j.seppur.2013.12.020.

[16] M.A.S. Rodrigues, C. Korzenovski, E. Gondran, A.M. Bernardes, J.Z. Ferreira, Evaluation of changes on ion-selective membranes in contact with zinc-cyanide complexes, J. Memb. Sci. 279 (2006) 140–147, https://doi.org/10.1016/j.memsci.2005.11.045.

[17] W. Garcia-Vasquez, L. Dammak, C. Larchet, V. Nikonenko, D. Grande, Effects of acid-base cleaning procedure on structure and properties of anion-exchange membranes used in electrodialysis, J. Memb. Sci. 507 (2016) 12–23, https://doi.org/10.1016/j.memsci.2016.02.006.

[18] M.C. Martí-Calatayud, D.C. Buzzi, M. García-Gabaldón, A.M. Bernardes, J.A.S. Tenório, V. Pérez-Herranz, Ion transport through homogeneous and heterogeneous ion-exchange membranes in single salt and multicomponent electrolyte solutions, J. Memb. Sci. 466 (2014) 45–57, https://doi.org/10.1016/j.memsci.2014.04.033.

[19] T. Sata, M. Tsujimoto, T. Yamaguchi, K. Matsusaki, Change of anion Exchange membranes in an aqueous sodium hydroxide solution at high temperature, J. Memb. Sci. 112 (1996) 161–170, https://doi.org/10.1016/0376-7388(95)00292-8.

[20] G. Merle, M. Wessling, K. Nijmeijer, Anion exchange membranes for alkaline fuel cells: a review, J. Memb. Sci. 377 (2011) 1–35, https://doi.org/10.1016/j.memsci.2011.04.043.

[21] G. Couture, A. Alaaeddine, F. Boschet, B. Ameduri, Progress in polymer Science polymeric materials as anion-exchange membranes for alkaline fuel cells, Prog. Polym. Sci. 36 (2011) 1521–1557, https://doi.org/10.1016/j.progpolymsci.2011.04.004.

[22] R.K. Nagarale, G.S. Gohil, V.K. Shahi, Recent developments on ion-exchange membranes and electro-membrane processes, Adv. Colloid Interf. Sci. 119 (2006) 97–130, https://doi.org/10.1016/j.cis.2005.09.005.

[23] J.H. Choi, S.H. Moon, Structural change of ion-exchange membrane surfaces under high electric fields and its effects on membrane properties, J. Colloid Interface Sci. 265 (2003) 93–100, https://doi.org/10.1016/S0021-9797(03)00136-X.

[24] M.C. Martí-Calatayud, M. García-Gabaldón, V. Pérez-Herranz, E. Ortega, Determination of transport properties of Ni(II) through a nafion cation-exchange membrane in chromic acid solutions, J. Memb. Sci. 379 (2011) 449–458, https://doi.org/10.1016/j.memsci.2011.06.014.

[25] R. Ibanez, D.F. Stamatialis, M. Wessling, Role of membrane surface in concentration polarization at cation exchange membranes, J. Memb. Sci. 239 (2004) 119–128, https://doi.org/10.1016/j.memsci.2003.12.032.

[26] R. Ghalloussi, W. Garcia-vasquez, L. Chaabane, L. Dammak, C. Larchet, S.V. Deabate, Ageing of ion-exchange membranes in electrodialysis: a structural and physicochemical investigation, J. Memb. Sci. 436 (2013) 68–78, https://doi.org/10.1016/j.memsci.2013.02.011.

[27] V.V. Gil, M.A. Andreeva, L. Jansezian, J. Han, N.D. Pismenskaya, V.V. Nikonenko, C. Larchet, L. Dammak, Impact of heterogeneous cation-exchange membrane surface modification on chronopotentiometric and current–voltage characteristics in NaCl, CaCl2 and MgCl2 solutions, Electrochim. Acta 281 (2018) 472–485,

https://doi.org/10.1016/j.electacta.2018.05.195.

[28] M.A. Andreeva, V.V. Gil, N.D. Pismenskaya, L. Dammak, N.A. Kononenko, C. Larchet, D. Grande, V.V. Nikonenko, Mitigation of membrane scaling in electrodialysis by electroconvection enhancement, pH adjustment and pulsed electric field application, J. Memb. Sci. 549 (2018) 129–140, https://doi.org/10.1016/j.memsci.2017.12.005.

[29] N. Pismenskaia, P. Sistat, P. Huguet, V. Nikonenko, G. Pourcelly, Chronopotentiometry applied to the study of ion transfer through anion Exchange membranes, J. Memb. Sci. 228 (2004) 65–76, https://doi.org/10.1016/j.memsci.2003.09.012.

[30] M.C. Martí-Calatayud, M. García-Gabaldón, V. Pérez-Herranz, Effect of the equilibria of multivalent metal sulfates on the transport through cation-exchange membranes at different current regimes, J. Memb. Sci. 443 (2013) 181–192, https://doi.org/10.1016/j.memsci.2013.04.058.

[31] E. Belova, G. Lopatkova, N. Pismenskaya, V. Nikonenko, C. Larchet, Role of water splitting in development of electroconvection in ion-exchange membrane systems, Desalination. 199 (2006) 59–61, https://doi.org/10.1016/j.desal.2006.03.142.

[32] A.C. Cope, E.R. Trumbull, Olefins from amines: the hofmann elimination reaction and amine oxide pyrolysis, Org. React. John Wiley & Sons, Inc., 2004, , https://doi.org/10.1002/0471264180.or011.05.

[33] M. Kuć, K. Cieślik-Boczula, P. Świątek, A. Jaszczyszyn, K. Gąsiorowski, W. Malinka, FTIR-ATR study of the influence of the pyrimidine analog of fluphenazine on the chain-melting phase transition of sphingomyelin membranes, Chem. Phys. 458 (2015) 9–17, https://doi.org/10.1016/j.chemphys.2015.06.010.

[34] D. Kołodyńska, Z. Hubicki, S. Pasieczna-Patkowska, FT-IR/PAS studies of Cu(II)-EDTA complexes sorption on the chelating ion exchangers, Acta Phys. Pol. A. 116 (2009) 340–343, https://doi.org/10.12693/APhysPolA.116.340.

[35] D.T. Sawyer, J.M. McKinnie, Properties and infrared spectra of ethylenediaminetetraacetic acid complexes. II. Chelates of divalent ions, J. Am. Chem. Soc. 82 (1960) 4191–4196, https://doi.org/10.1021/ja01501a019.

[36] J. Cheng, X. Yang, L. Dong, Z. Yuan, W. Wang, S. Wu, S. Chen, G. Zheng, W. Zhang, D. Zhang, H. Wang, Effective nondestructive evaluations on UHMWPE/recycled- PA6 blends using FTIR imaging and dynamic mechanical analysis, Polym. Test. 59 (2017) 371–376, https://doi.org/10.1016/j.polymertesting.2017.02.021.

[37] M. Grochowicz, A. Kierys, TG/DSC/FTIR studies on the oxidative decomposition of polymer-silica composites loaded with sodium ibuprofen, Polym. Degrad. Stab. 138 (2017) 151–160, https://doi.org/10.1016/j.polymdegradstab. 2017.03.007.

[38] M.F.G. Esteban, R.V. Serrano, F.G. Vilchez, Synthesis and vibrational study of some polydentate ligands, Spectrochim. Acta Part A Mol. Spectrosc. 43 (1987) 1039–1043, https://doi.org/10.1016/0584-8539(87)80176-9.

[39] S. Srinivasan, S. Gunasekaran, U. Ponnambalam, A. Savarianandam, S. Gnanaprakasam, S. Natarajan, Spectroscopic and thermodynamic analysis of enolic form of 3-oxo-L-gulofuranolactone, Indian J. Pure Appl. Phys. 43 (2005) 459–462, https://doi.org/10.1109/TNSRE.2018.2843884.

[40] Y. Hosakun, K. Halász, M. Horváth, L. Csóka, V. Djoković, ATR-FTIR study of the interaction of CO2 with bacterial cellulose-based membranes, Chem. Eng. J. 324 (2017) 83–92, https://doi.org/10.1016/j.cej.2017.05.029.

[41] K.C. Lanigan, K. Pidsosny, Reflectance FTIR spectroscopic analysis of metal complexation to EDTA and EDDS, Vib. Spectrosc. 45 (2007) 2–9, https://doi.org/10.1016/j.vibspec.2007.03.003.

[42] W. Garcia-Vasquez, R. Ghalloussi, L. Dammak, C. Larchet, V. Nikonenko, D. Grande, Structure and properties of heterogeneous and homogeneous ion-exchange membranes subjected to ageing in sodium hypochlorite, J. Memb. Sci. 452 (2014) 104–116, https://doi.org/10.1016/j.memsci.2013.10.035.

[43] S. Caprarescu, A.-L. Radu, V. Purcar, R. Ianchis, A. Sarbu, M. Ghiurea, C. Nicolae, C. Modrogan, D.-I. Vaireanu, A. Périchaud, D.-I. Ebrasu, Adsorbents/ion exchangers-PVA blend membranes: preparation, characterization and performance for the removal of Zn2+ by electrodialysis, Appl. Surf. Sci. 329 (2015) 65–75, https://doi.org/10.1016/j.apsusc.2014.12.128.

[44] S. Caprarescu, M.C. Corobea, V. Purcar, C.I. Spataru, R. Ianchis, G. Vasilievici, Z.

Vuluga, San copolymer membranes with ion exchangers for Cu(II) removal from synthetic wastewater by electrodialysis, J. Environ. Sci. (China) 35 (2015) 27–37, https://doi.org/10.1016/j.jes.2015.02.005.

[45] P. Hébert, A. Le Rille, W.Q. Zheng, A. Tadjeddine, Vibrational spectroscopic study of the adsorption of pyridine at the Au(111)-electrolyte interface by in situ difference frequency generation, J. Electroanal. Chem. 447 (1998) 5–9, https://doi.org/10.1016/S0022-0728(98)00035-7.

[46] K. Nakanishi, P.H. Solomon, Infrared Absorption Spectroscopy, 2d ed, Holden-Day, San Francisco, 1977.

[47] V.V. Nikonenko, A.V. Kovalenko, M.K. Urtenov, N.D. Pismenskaya, J. Han, P. Sistat, G. Pourcelly, Desalination at overlimiting currents: state-of-the-art and perspectives, Desalination. 342 (2014) 85–106, https://doi.org/10.1016/j.desal.2014.01.008.

[48] F.D.R. Amado, M.A.S. Rodrigues, F.D.P. Morisso, A.M. Bernardes, J.Z. Ferreira, C.A. Ferreira, High-impact polystyrene/polyaniline membranes for acid solution treatment by electrodialysis: preparation, evaluation, and chemical calculation, J. Colloid Interface Sci. 320 (2008) 52–61, https://doi.org/10.1016/j.jcis.2007.11.054.

[49] L. Benavente, C. Coetsier, A. Venault, Y. Chang, C. Causserand, P. Bacchin, P. Aimar, FTIR mapping as a simple and powerful approach to study membrane coating and fouling, J. Memb. Sci. 520 (2016) 477–489, https://doi.org/10.1016/j.memsci.2016.07.061.

[50] C. Wang, X. Bai, S. Liu, L. Liu, Synthesis of cobalt-aluminum spinels via EDTA chelating precursors, J. Mater. Sci. 39 (2004) 6191–6201, https://doi.org/10.1023/b:jmsc.0000043586.66653.de.

[51] K.H. Wu, Y.R. Wang, W.H. Hwu, FTIR and TGA studies of poly (4-vinylpyridine-codivinylbenzene)– Cu (II) complex, Polym. Degrad. Stab. 79 (2003) 195–200.

[52] Ž. Mitić, M. Cakić, G. Nikolić, Fourier-transform IR spectroscopic investigations of cobalt(II)-dextran complexes by using D2O isotopic exchange, Spectroscopy. 24 (2010) 269–275, https://doi.org/10.3233/SPE-2010-0467.

[53] Q. Xia, X.J. Zhao, S.J. Chen, W.Z. Ma, J. Zhang, X.L. Wang, Effect of solution blended poly(styrene-co-acrylonitrile) copolymer on crystallization of poly(vinylidene fluoride), Express Polym Lett 4 (2010) 284–291, https://doi.org/10.3144/expresspolymlett.2010.36.

[54] E.N. Komkova, D.F. Stamatialis, H. Strathmann, M. Wessling, Anion-exchange membranes containing diamines: preparation and stability in alkaline solution, J. Memb. Sci. 244 (2004) 25–34, https://doi.org/10.1016/j.memsci.2004.06.026.

[55] L. Dammak, C. Larchet, D. Grande, Ageing of ion-exchange membranes in oxidant solutions, Sep. Purif. Technol. 69 (2009) 43–47, https://doi.org/10.1016/j.seppur.2009.06.016.

[56] P. Bulejko, K. Weinertová, Properties and structure of heterogeneous ion-exchange membranes after exposure to chemical agents, J. Solid State Electrochem. 21 (2017) 111–124, https://doi.org/10.1007/s10008-016-3341-1.